

Synthesis of an Uncharged Tetra-cyclopeptide Acting as a Transmembrane Carrier: Enhanced Cellular and Nuclear Uptake

Flaviane Francisco Hilário,^{†,‡,§} Mohamed Dit Mady Traoré,^{†,||} Vincent Zwick,[⊥] Laurence Berry,[#] Claudia A. Simões-Pires,[⊥] Muriel Cuendet,[⊥] Nicolas Fantozzi,[†] Rossimiriam Pereira de Freitas,[§] Marjorie Maynadier,[#] Sharon Wein,[#] Henri Vial,[#] and Yung-Sing Wong^{*,†,||}

[†]Univ. Grenoble Alpes, Département de Pharmacochimie Moléculaire, CNRS UMR 5063, ICMG FR 2607, 470 rue de la chimie, Grenoble 38041 Cedex 9, France

[‡]Universidade Federal de Ouro Preto, Departamento de Química, ICEB, Campus Universitário Morro do Cruzeiro, 35400-000 Ouro Preto, Minas Gerais Brazil

[§]Universidade Federal de Minas Gerais, Departamento de Química, UFMG, Av Pres Antônio Carlos, 6627, Pampulha, Belo Horizonte, MG 31270-901, Brazil

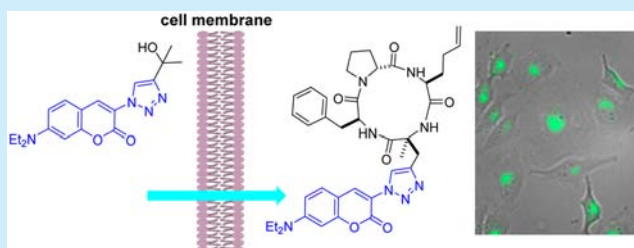
^{||}Univ. Grenoble Alpes, Département de Chimie Moléculaire, CNRS UMR 5250, ICMG FR 2607, 301 rue de la chimie, Grenoble 38041 Cedex 9, France

[⊥]School of Pharmaceutical Sciences, University of Geneva, University of Lausanne, rue Michel Servet 1, 1211 Geneva, Switzerland

[#]Laboratoire Dynamique des Interactions Membranaires Normales et Pathologiques, UMR5235, CNRS, University of Montpellier, Place Eugène Bataillon, 34095 Montpellier, France

Supporting Information

ABSTRACT: A small uncharged cyclopeptide scaffold inspired by a natural product and designed to undergo postfunctionalizations was used as a new transmembrane vector. A bioactive and fluorescent triazole aminocoumarin was bound to this carrier to facilitate its moving across cell and subcellular membranes, and this led to an increase in its cell toxicity.



Most bioactive molecules need to overcome cellular membrane barriers to accomplish their therapeutic action. In this context, cell-penetrating peptides (CPPs), as a transmembrane vector, have proven to be particularly efficient in facilitating cell penetration for small to large cargos.¹ A number of currently developed CPPs are structurally related to cationic peptides like the Tat sequence, which is derived from the protein transduction domain in the HIV-1 virus transcriptional factor.² These peptides are able to enter cells by interacting with the negatively charged cell membrane followed by endocytosis or direct translocation. Besides related issues of serum binding or nonspecific interaction with other charged intracellular compartments, the endosomal internalization mechanism can complicate the release of bioactive compounds into the cytoplasm. Cyclization of cationic peptides can improve enzymatic stability and cell permeability³ and has resulted in endosomal escape⁴ and nuclear-targeting⁵ capacities. Meanwhile, recent efforts have been carried out to decipher the mechanism of cell permeability of uncharged small cyclic peptides inspired by natural products.⁶ Such structures were able to cross membranes in a passive manner⁷ and had in a few cases better oral bioavailability.⁸ This passive membrane permeability could be explained by the free energy cost reduction of backbone amide desolvation upon

moving from a polar solvent-exposed environment to membrane. This process involves the formation of internal hydrogen bonds from a backbone amide that easily modulate the cyclopeptide conformation to adapt to the medium.⁷ For the hexa-cyclopeptide templates, modification of side-chain lipophilicity was reported to influence membrane permeability,^{6,9} and recent investigations have shown tolerance for hydrophilic substitution with hexapeptomer.¹⁰

Recently, we have been involved in the synthesis of new analogues¹¹ of the natural product FR235222¹² (Figure 1). FR235222 and **1** were highly bioactive in cell assays and can be divided into two structural parts, the tetra-cyclopeptide that could be responsible for cell permeability and the zinc binding group involved in histone deacetylase (HDAC) inhibitor activity. Its small cyclic peptide structure shares common features with other uncharged small cyclic peptides having passive membrane permeability properties. Based on these assessments, we wondered if such a small tetra-cyclopeptide scaffold could improve the property of a small bioactive molecule to cross many

Received: December 19, 2016

Published: January 20, 2017

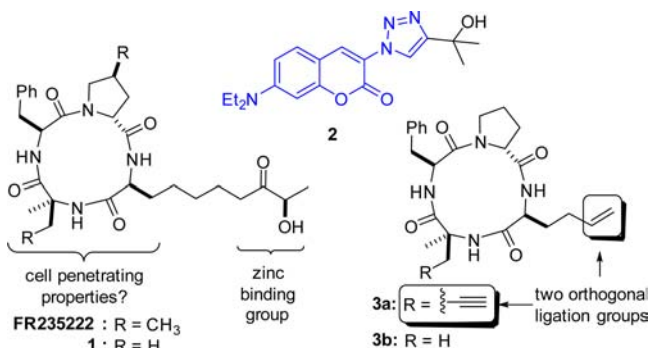


Figure 1. Natural product FR235222, the bioactive and fluorescent model compound **1**, and the modular tetra-cyclopeptide cell permeable vector **2**.

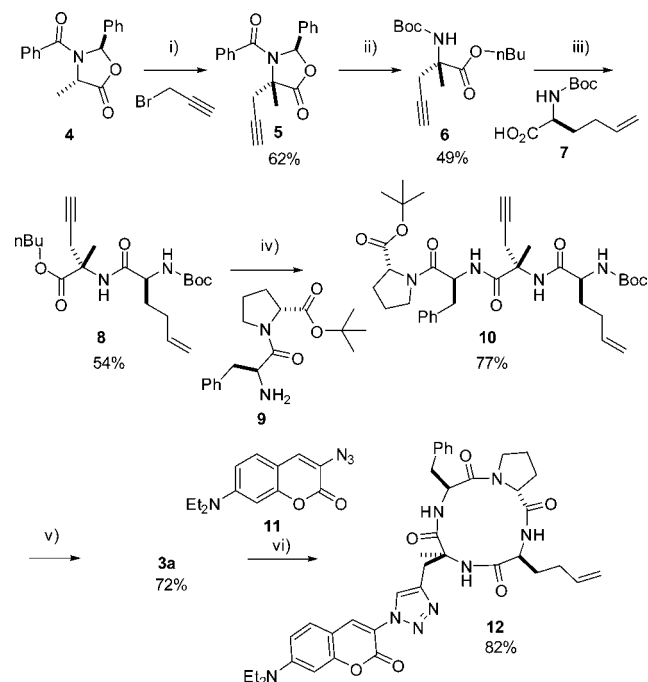
barriers like cell and nuclear membranes. To this end, a direct evaluation in live cell conditions is reported.

To monitor these events, the triazole aminocoumarin group¹³ (shown on the product **2** in blue) was selected as the pharmacophore and cargo. This simple pharmacophore has many advantages in this study. It can be traced in cells as a fluorescent molecule¹³ and was recently identified by some of us¹⁴ to induce reactive oxygen species (ROS) in *Cryptococcus*. Once coupled to a cationic peptide, the resulting product was active against various *Cryptococcus* strains. Structurally, its molecular weight (ca. 300 g·mol⁻¹) remains smaller than the cyclopeptide vector (ca. 450 g·mol⁻¹). In practice, the ligation to the vector can be conveniently made by a simple click reaction. By virtue of its high cell permeability, the resulting product is expected to cause higher intracellular concentration of the triazole aminocoumarin pharmacophore that could ultimately lead to improved bioactivity.

A bivalent tetra-cyclopeptide **3a** was designed to keep the central core as close as possible to the natural product FR235222 with a terminal alkyne and an olefin group placed on the side chains, allowing modular ligation with two orthogonal reactive groups. The corresponding protected amino ester **6** was obtained according to the Seebach and Mutter procedures¹⁵ starting from the crystalline chiral synthon **4**¹⁶ (Scheme 1). Alkylation of the lithium enolate of **4** with propargyl bromide provided **5** as a single diastereoisomer after recrystallization. Acidic hydrolysis, followed by subsequent *N*-Boc protection and esterification with *n*-butanol, afforded the amino ester **6** in an overall yield of 49%. Condensation with the *N*-Boc-homoallylglycine **7**¹¹ gave the dipeptide **8**, which in turn, was coupled with the dipeptide **9** to yield the linear tetrapeptide **10**. After deprotection and cyclization, the key tetra-cyclopeptide **3a** was obtained in a good yield of 72%. This synthetic sequence is amenable to transfer to solid-phase peptide synthesis that would allow more straightforward generation of focused or combinatorial libraries. Having the compound **3a** in hand, the cyclopeptide triazole aminocoumarin **12** was made by the coupling of the azidocoumarin **11** to **3a** using a copper-catalyzed Huisgen reaction. The use of polymer-supported Amberlyst-A21/CuI catalyst¹⁷ gave the fluorescent product **12** in reproducible yields.

The antiproliferative activity of the triazole aminocoumarin **2** and the tetra-cyclopeptide vector alone **3b**¹¹ were first evaluated on human cancer cell lines (Jurkat, HeLa) and HEK 293 immortalized cells (see the Supporting Information, Table 2) to select the best experimental conditions for the fluorescence microscopy (no cell toxicity). *P. falciparum* was selected as being an intracellular parasite and was used as a model possessing an

Scheme 1. Synthesis of Tetra-cyclopeptide Intermediate **12**^a



^aConditions: (i) LiN(TMS)₂, THF, -78 °C; (ii) (a) concd HCl, 115 °C, 2.5 h, (b) TMSCl, *n*BuOH, 70 °C, overnight, (c) (Boc)₂O, Et₃N, rt, overnight; (iii) (a) TFA, CH₂Cl₂, (b) **7**, DCC, HOBT, Et₃N, DMF; (iv) (a) LiOH, THF, MeOH, 8 h, 40 °C, (b) **9**, DCC, HOBT, Et₃N, DMF; (v) (a) TFA, 0 °C, 3 h, (b) HATU, DIEA, DMF, overnight; (vi) Amberlyst-A21 CuI cat., CH₂Cl₂, rt, 24 h.

additional cell membrane (host cell). No toxicity was detected for **3b** (IC₅₀ > 100 μM), while **2** was found to affect cell proliferation only on Jurkat in human cells and on *P. falciparum* with a weak IC₅₀ of 41.8 and 43.4 μM, respectively.

The cell-permeability properties of the fluorescent probes **2** and of **12** were then compared using HeLa cells, monitored by a simple cell microplate imager (Figure 2).

Cells treated with **12** exhibited a rapid cell fluorescence labeling, whereas the fluorochrome **2** alone was poorly permeable and was not visible inside the cells after 15 min of treatment. Evidence of intracellular localization was provided by the heterogeneous distribution of **12** inside the cell where high fluorescence signals were located at the perinuclear area without

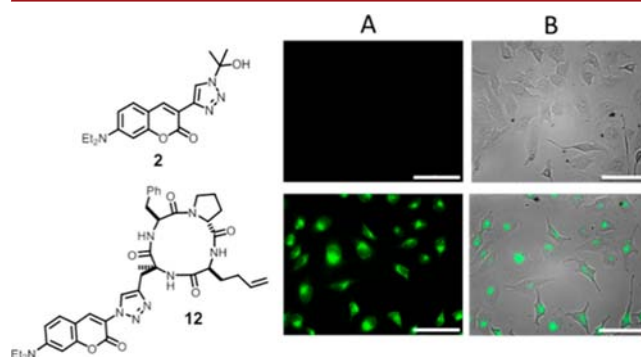
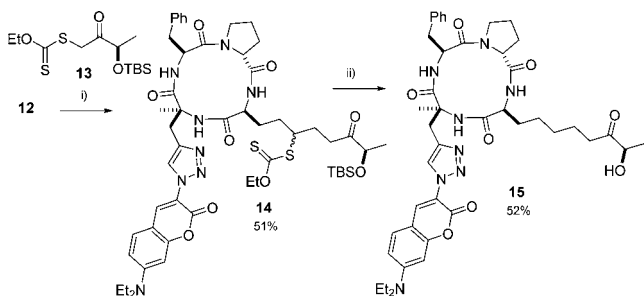


Figure 2. Global cell distribution of compounds **2** and **12**. Conditions: HeLa cells were incubated with 2.5 μM compounds **2** and **12** for 15 min at 37 °C. (A) Images collected with a microplate cell imager using a GFP filter. (B) Merged image GFP filter/bright field. Scale bar: 100 μm.

labeling the nucleus and the cytoplasm. This preferential organelle labeling from fluorescent triazole aminocoumarins had already been observed¹⁸ and may constitute an obstacle for further evaluation of subcellular membrane permeability like the nucleus. To overcome this limitation, the α -hydroxyl ketone zinc binding group, hence acting as an addressing motif for the nucleus, was added to this tetra-cyclopeptide to better evaluate the nuclear entrance. Indeed, HDAC inhibitors (HDACi's) bearing a ketone zinc binding group have been described to confer selective inhibitions toward nuclear HDACs¹⁹ and are thus prone to localize in this cell compartment. With this additional motif on the cyclopeptide scaffold, a significant increase in probe concentration inside the nucleus is thus expected. The addition of the α -hydroxyl ketone zinc binding group was achieved by assembling the xanthate **13** with **12** according to the Zard's radical coupling reaction²⁰ to yield the xanthate **14** (Scheme 2). A concomitant xanthate reduction/silyl deprotection using $\text{H}_3\text{PO}_2/\text{Et}_3\text{N}$ reagents²¹ provided the fluorescent tetra-cyclopeptide **15** in a single step.

Scheme 2. Synthesis of Tetra-cyclopeptide **15**^a



^aConditions: (i) dilauroyl peroxide, $\text{ClCH}_2\text{CH}_2\text{Cl}$, 175 °C, overnight; (ii) $\text{H}_3\text{PO}_2/\text{Et}_3\text{N}$, AIBN, dioxane, 145 °C, 2 h.

To increase the sensitivity and the resolution, an upright fluorescence microscope set with a high-resolution 100 \times objective was used to localize compounds **12** and **15** more precisely. HeLa cells were stained with Draq5 to visualize the DNA (Figure 3). Due to the small depth of field with high-resolution objectives, the visualization of the whole cell in the depth with a single image was not possible. Using a deep focus (focal plane nearby the support), the outline of the cells could be visualized under white light illumination in the differential interference contrast (DIC) (Figure 3A). Compounds **12** and **15** clearly accumulated at specific intracellular organelles confirming their cell internalization in live cell conditions. This was particularly clear when looking at the large pseudopodia of the cells (black arrows) devoid of labeling. When focusing on the nucleus (Figure 3B), compound **15** was clearly visible inside the nucleus, although the major part still localized perinuclearly. These results provide evidence that the fluorescent cargo coupled to the cyclopeptide vector **15** was able to cross the nuclear envelope and suggest that its zinc-binding motif contributed to the selective nuclear location and retention. Noteworthy, unlike most fluorescent nuclear staining agents, **15** does not seem to label the DNA as nucleoli appeared as black holes in nuclei, indicating that the compound is concentrated in the nucleoplasm, where HDACi's are known to affect transcriptional regulation.²²

The HDAC activity of **15** was evaluated and compared with the other probes to see whether this additional specific location in the nucleus correlated well with an activity and selectivity

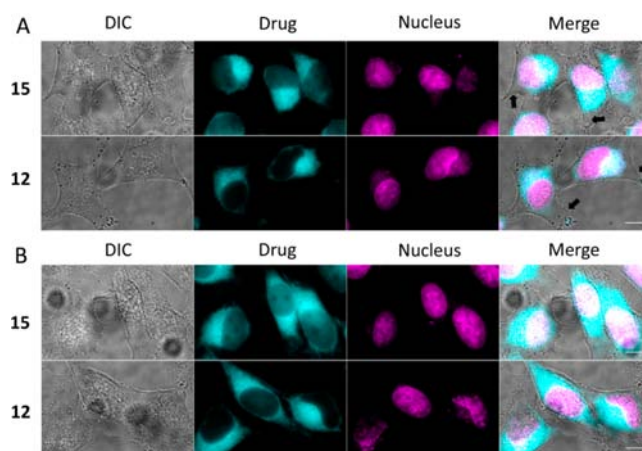


Figure 3. Cell distribution of compounds **12** and **15** under live cell microscopy conditions. Conditions: HeLa cells were incubated with 160 nM compounds **12** and **15** for 1 h at 37 °C. Cells were stained with Draq5 to visualize the DNA. (A) Selected cells imaged at a deep focal plane to visualize pseudopodia (black arrows) and the localization of **12** and **15**. (B) Selected cells imaged at the nucleus focal plane showing the intranuclear staining with compound **15** and not with compound **12**. Scale bar: 10 μm .

toward nuclear class I HDACs. As **2**, **12**, and **15** are fluorescent compounds, an HDAC inhibition assay using MS detection was applied to determine their potency and their selectivity.²³ Compound **1** and the analogue **15** with the cargo showed a high inhibitory efficiency against HDAC using a HeLa nuclear extract (IC_{50} = 8.4 and 35.8 nM, respectively), while no effect was detected against HDAC6 (IC_{50} > 300 μM), a class IIb HDAC mainly localized in cytoplasm (see the Supporting Information, Table 1). The simple tetra-cyclopeptide scaffold **3b**, the cargo coupled with the tetra-cyclopeptide without zinc binding group **12**, and compound **2** were not active on both enzymatic assays (IC_{50} > 300 μM).

The antiproliferative activity of **1**, **12**, and **15** was further evaluated against *P. falciparum*, the two cancer cell lines, and HEK293 immortalized cells (see the Supporting Information, Table 2). Due to its additional HDAC inhibitor effect, the product **15** proved to affect proliferation in all cell lines (*P. falciparum*: IC_{50} = 0.919 μM ; Jurkat: IC_{50} = 1.67 μM ; HeLa: IC_{50} = 0.56 μM ; HEK293: IC_{50} = 0.27 μM) while remaining less potent than **1** (*P. falciparum*: IC_{50} = 0.017 μM ; Jurkat: IC_{50} = 0.048 μM ; HeLa: IC_{50} = 0.17 μM ; HEK293: IC_{50} = 0.04 μM). This may be due to the partial retention of **15** in the perinuclear envelope, lowering its concentration in the nucleus (Figure 3B).

With regard to the triazole aminocoumarin pharmacophore, it is interesting to note that its tetra-cyclopeptide version (**12**) compared to **2** exhibited a 2.7–35-fold increase of bioactivity against Jurkat and *P. falciparum* (IC_{50} of 15.6 and 1.24 μM , respectively). HeLa and HEK293 cells remained unaffected by **12** (IC_{50} > 100 μM) indicating a possible lesser sensitivity to ROS activator. These results illustrate the ability of the tetra-cyclopeptide scaffold to increase the cell permeability of the triazole aminocoumarin resulting in an increase of cell toxicity.

In conclusion, we have synthesized a bivalent tetra-cyclopeptide inspired by the natural product FR235222 as a new transmembrane vector devoted to enhance cell permeation of small bioactive compounds. Using the triazole aminocoumarin as a cargo model, an increase in cell permeability and toxicity was achieved. Adding an addressing motif for nucleus to this cyclopeptide scaffold offered a better view of its ability to cross

nuclear membrane with the cargo. Since it is covalently bound, the triazole aminocoumarin group constitutes a substantial part of compound **12**, and its position on the amino acid residue does not appear to compromise the cell-penetrating property. This work represents a distinct use of a small uncharged cyclopeptide acting as a transmembrane vector. Further work will be necessary to identify the functional and structural determinants that will retain, impair, or improve the cell-membrane permeability of this tetra-cyclopeptide scaffold.

■ ASSOCIATED CONTENT

■ Supporting Information

The Supporting Information is available free of charge on the ACS Publications website at DOI: [10.1021/acs.orglett.6b03776](https://doi.org/10.1021/acs.orglett.6b03776).

Biological assay conditions, experimental procedures, and full spectroscopic data for all new compounds (PDF)

■ AUTHOR INFORMATION

Corresponding Author

*E-mail: yung-sing.wong@univ-grenoble-alpes.fr.

ORCID

Yung-Sing Wong: 0000-0003-1038-9681

Notes

The authors declare no competing financial interest.

■ ACKNOWLEDGMENTS

Financial supports by "Agence Nationale de la Recherche" under "programme Labex" (ARCANE Project No. ANR-11-LABX-003), "fondation pour le développement de la chimie des substances naturelles et ses applications" Institut de France/Académie des Sciences, and CNRS are gratefully acknowledged. Financial support from the Swiss National Science Foundation (P300P3 158507) and the Pierre Mercier Foundation is also acknowledged. F.F.H. was supported by a fellowship (PDSE 9712-11-9) from the CAPES Foundation (Coordenação de Aperfeiçoamento de Pessoal de Nível Superior), Ministry of Education of Brazil. The Brazilian agencies FAPEMIG, CNPq, and CAPES are acknowledged for fellowships to F.F.H. and R.P.d.F. The *P. falciparum* 3D7 strain was obtained through the Malaria Research and Reference Reagent Resource Center (MR4; www.beiresources.org). We thank Vicky Diakou from the Montpellier RIO imaging facility of the MRI-DBS University of Montpellier for her assistance. ICMG (Institut de Chimie Moléculaire de Grenoble) Chemistry Nanobio Platform is acknowledged for analysis and characterization facilities.

■ REFERENCES

- (1) (a) Ramsey, J. D.; Flynn, N. H. *Pharmacol. Ther.* **2015**, *154*, 78. (b) Kauffman, W. B.; Fuselier, T.; He, J.; Wimley, W. C. *Trends Biochem. Sci.* **2015**, *40*, 749. (c) Reissmann, S. *J. Pept. Sci.* **2014**, *20*, 760. (d) Bechara, C.; Sagan, S. *FEBS Lett.* **2013**, *587*, 1693. (e) Stanzl, E. G.; Trantow, B. M.; Vargas, J. R.; Wender, P. A. *Acc. Chem. Res.* **2013**, *46*, 2944. (f) Milletti, F. *Drug Discovery Today* **2012**, *17*, 850.
- (2) (a) Green, M.; Loewenstein, P. M. *Cell* **1988**, *55*, 1179. (b) Frankel, A. D.; Pabo, C. O. *Cell* **1988**, *55*, 1189.
- (3) (a) Horne, W. S.; Wiethoff, C. M.; Cui, C.; Wilcoxon, K. M.; Amorin, M.; Ghadiri, M. R.; Nemerow, G. R. *Bioorg. Med. Chem.* **2005**, *13*, 5145. (b) Lättig-Tünnemann, G.; Prinz, M.; Hoffmann, D.; Behlke, J.; Palm-Apergi, C.; Morano, I.; Herce, H. D.; Cardoso, M. C. *Nat. Commun.* **2011**, *2*, 453. (c) Qian, Z.; Liu, T.; Liu, Y.-Y.; Briesewitz, R.; Barrios, A. M.; Jhian, S. M.; Pei, D. *ACS Chem. Biol.* **2013**, *8*, 423. (d) Shapira, R.; Rudnick, S.; Daniel, B.; Viskind, O.; Aisha, V.; Richman,

M.; Ayasolla, K. R.; Perelman, A.; Chill, J. H.; Gruzman, A.; Rahimpour, S. *J. Med. Chem.* **2013**, *56*, 6709. (e) Traboulsi, H.; Larkin, H.; Bonin, M. A.; Volkov, L.; Lavoie, C. L.; Marsault, E. *Bioconjugate Chem.* **2015**, *26*, 405.

(4) (a) Qian, Z.; LaRochelle, J. R.; Jiang, B.; Lian, W.; Hard, R. L.; Selner, N. G.; Luechapanichkul, R.; Barrios, A. M.; Pei, D. *Biochemistry* **2014**, *53*, 4034. (b) Qian, Z.; Martyna, A.; Hard, R. L.; Wang, J.; Appiah-Kubi, G.; Coss, C.; Phelps, M. A.; Rossman, J. S.; Pei, D. *Biochemistry* **2016**, *55*, 2601.

(5) Mandal, D.; Nasrolahi Shirazi, A.; Parang, K. *Angew. Chem., Int. Ed.* **2011**, *50*, 9633.

(6) Hewitt, W. M.; Leung, S. S. F.; Pye, C. R.; Ponkey, A. R.; Bednarek, M.; Jacobson, M. P.; Lokey, R. S. *J. Am. Chem. Soc.* **2015**, *137*, 715.

(7) (a) Rezaei, T.; Yu, B.; Millhauser, G. L.; Jacobson, M. P.; Lokey, R. S. *J. Am. Chem. Soc.* **2006**, *128*, 2510. (b) Rezaei, T.; Bock, J. E.; Zhou, M. V.; Kalyanaraman, C.; Lokey, R. S.; Jacobson, M. P. *J. Am. Chem. Soc.* **2006**, *128*, 14073. (c) Wang, C. K.; Northfield, S. E.; Swedberg, J. E.; Colless, B.; Chaousis, S.; Price, D. A.; Liras, S.; Craik, D. J. *Eur. J. Med. Chem.* **2015**, *97*, 202.

(8) Nielsen, D. S.; Hoang, H. N.; Lohman, R.-J.; Hill, T. A.; Lucke, A. J.; Craik, D. J.; Edmonds, D. J.; Griffith, A. A.; Rotter, C. J.; Ruggeri, R. B.; Price, D. A.; Liras, S.; Fairlie, D. P. *Angew. Chem., Int. Ed.* **2014**, *53*, 12059.

(9) Thansandote, P.; Harris, R. M.; Dexter, H. L.; Simpson, G. L.; Pal, S.; Upton, R. J.; Valko, K. *Bioorg. Med. Chem.* **2015**, *23*, 322.

(10) Furukawa, A.; Townsend, C. E.; Schwachert, J.; Pye, C. R.; Bednarek, M. A.; Lokey, R. S. *J. Med. Chem.* **2016**, *59*, 9503.

(11) Traoré, M.; Mietton, F.; Maubon, D.; Peuchmaur, M.; Francisco Hilário, F.; Pereira de Freitas, R.; Bougdour, A.; Curt, A.; Maynadier, M.; Vial, H.; Pelloux, H.; Hakimi, M.-A.; Wong, Y.-S. *J. Org. Chem.* **2013**, *78*, 3655.

(12) Mori, H.; Urano, Y.; Kinoshita, T.; Yoshimura, S.; Takase, S.; Hino, M. *J. Antibiot.* **2003**, *56*, 181.

(13) Sivakumar, K.; Xie, F.; Cash, B. M.; Long, S.; Barnhill, H. N.; Wang, Q. *Org. Lett.* **2004**, *6*, 4603.

(14) Ferreira, S. Z.; Carneiro, H. C.; Lara, H. A.; Alves, R. B.; Resende, J. M.; Oliveira, H. M.; Silva, L. M.; Santos, D. A.; Pereira de Freitas, R. *ACS Med. Chem. Lett.* **2015**, *6*, 271.

(15) (a) Seebach, D.; Naef, R. *Helv. Chim. Acta* **1981**, *64*, 2704. (b) Nebel, K.; Mutter, M. *Tetrahedron* **1988**, *44*, 4793.

(16) Hsiao, Y.; Hegedus, L. S. *J. Org. Chem.* **1997**, *62*, 3586.

(17) Girard, C.; Onen, E.; Aufort, M.; Beauviere, S.; Samson, E.; Herscovici, J. *Org. Lett.* **2006**, *8*, 1689.

(18) (a) Zhou, Y.; Liu, K.; Li, J.-Y.; Fang, Y.; Zhao, T.-C.; Yao, C. *Org. Lett.* **2011**, *13*, 1290. (b) Ast, S.; Schwarze, T.; Mueller, H.; Sukhanov, A.; Michaelis, S.; Wegener, J.; Wolfbeis, O. S.; Koerzdoerfer, T.; Duerkop, A.; Holdt, H.-J. *Chem. - Eur. J.* **2013**, *19*, 14911.

(19) Bantscheff, M.; Hopf, C.; Savitski, M. M.; Dittmann, A.; Grandi, P.; Michon, A.-M.; Schlegl, J.; Abraham, Y.; Becher, I.; Bergamini, G.; Boesche, M.; Dellling, M.; Duempelfeld, B.; Eberhard, D.; Huthmacher, C.; Mathieson, T.; Poeckel, D.; Reader, V.; Strunk, K.; Sweetman, G.; Kruse, U.; Neubauer, G.; Ramsden, N. G.; Drewes, G. *Nat. Biotechnol.* **2011**, *29*, 255.

(20) Quiclet-Sire, B.; Zard, S. Z. *Chem. - Eur. J.* **2006**, *12*, 6002.

(21) Barton, D. H. R.; Jang, D. O.; Jaszberenyi, J. C. *Tetrahedron Lett.* **1992**, *33*, 5709.

(22) Lee, P.-C.; Wildt, D. E.; Comizzoli, P. *Biol. Reprod.* **2015**, *93*, 33.

(23) Zwick, V.; Simões-Pires, C.; Cuendet, M. *J. Enzyme Inhib. Med. Chem.* **2016**, *31*, 209.